THE JOURNAL OF PHYSICAL CHEMISTRY C

Article

Cite This: J. Phys. Chem. C 2019, 123, 7758−7765

pubs.acs.org/JPCC

Computational Study of Adsorption of CO_2, SO_2, and H_2CO on Free-Standing and Molybdenum-Supported CaO Films

Mikhail S. Kuklin,[†] Karoliina Honkala,[‡] and Hannu Häkkinen*[,†,‡]

[†]Department of Physics and [‡]Department of Chemistry, Nanoscience Center, University of Jyväskylä, FI-40014 Jyväskylä, Finland

Supporting Information

ABSTRACT: Oxide films play a significant role in a wide range of fields from catalysis to solar cell materials. CaO films are promising sorbents for many environmentally harmful molecules. Here, we report a systematic investigation of adsorption of CO_2, SO_2, and H_2CO on bulk and Mo-supported CaO(100) films using density functional theory. Significant effects on adsorption energy, charge transfer to the molecules, and degree of the C−O bond activation were demonstrated on Mo-supported CaO films by changing the film thickness, composition, and the strength and direction of an applied external electric field. These findings are relevant for interpreting results from scanning tunneling microscopy of small molecules on metal−supported oxide films and may be useful for better control of the properties of metal oxides, enabling a wide range of potential applications.

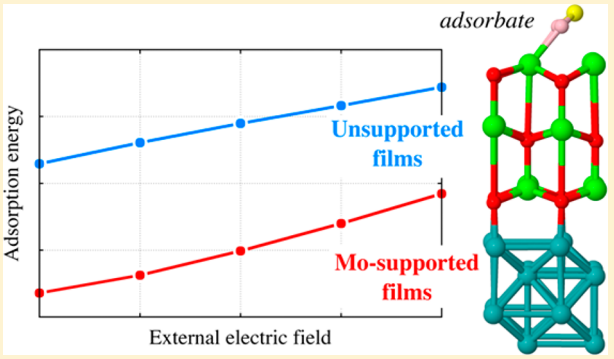

1. INTRODUCTION

Oxide materials are key components in a wide range of industrially relevant fields, such as heterogeneous catalysis, microelectronics, optoelectronics, spintronics, corrosion protection, solar energy materials, and tunneling magnetoresonance sensors.[1−5] One of the most prominent property of oxide films is electron transfer,[5] where oxide film thickness is a decisive factor for the mechanism of electron transport: a thin film, typically, promotes spontaneous electron tunneling while a thick film works through ballistic transport. This finding represents a unique feature of oxides and, in general, of other insulating materials that allows modifying their properties by changing film thickness, as oxides at the nanoscale typically exhibit different behavior compared to bulk material.[6] In particular, the effect of the thickness of MgO and CaO films on Au adsorption has been extensively studied by experimental and computational approaches. Electron tunneling through thin MgO films supported by metal was observed to provide negatively charged Au atoms and 2D clusters on the surface, whereas the effect becomes weaker with increasing film thickness.[4,5,7−10] In fact, CaO is isostructural to MgO representing a rocksalt material and, therefore, has similar properties such as the melting temperature and the band gap. A low Madelung potential renders CaO as a good electron donor.[11,12] The valence electrons of CaO are more delocalized as compared to MgO which leads to higher interaction of the surface with adsorbates. Therefore, interaction between CaO acid adsorbates such as carbon dioxide CO_2 and sulfur dioxide SO_2 is stronger than on MgO[13] and CaO can be used as a sorbent for environmentally harmful molecules.[14−16] CO_2 is a well-known greenhouse gas, but SO_2, is formed from burning sulfur-containing impurities in coals and petroleum, bringing adverse effects on a catalyst poisoning and equipment corrosion in oil-derived chemical feedstocks and contributing significantly to air pollution and smog.[17−19] Also a toxic organic compound, formaldehyde, induces environmental pollution. Therefore, significant efforts have been taken to transform these undesirable compounds to less harsh species and to achieve better control for environmental pollution and industrial processes including studies on characterization of sorbent properties of CaO surfaces.[14,15,20−22] While calcite ($CaCO_3$) formation on bulk CaO films was demonstrated both experimentally and computationally, the adsorption of, SO_2 and H_2CO have not been reported in literature, except on prototypical MgO. In particular, SO_3 formation was found on a MgO surface[23] and H_2CO adsorption was shown to lead to formate-like species via bonding between carbon of formaldehyde and oxygen of CaO layer.[24,25]

Recently, the effects of electric fields to CaO films were reported in literature demonstrating that they can be used to modify adsorption characteristics.[26] In particular, it was demonstrated that the band gap of CaO decreases in the presence of electric field and the effect is more pronounced on the thicker films. This is turn can directly influence adsorption due to the changes in the electronic structure of CaO films. Interestingly, manipulation of reactivity and morphology of a nanocatalyst structures by electric fields have been re-

Special Issue: Hans-Joachim Freund and Joachim Sauer Festschrift

Received: July 4, 2018
Revised: August 28, 2018
Published: September 3, 2018

DOI: 10.1021/acs.jpcc.8b06378
J. Phys. Chem. C 2019, 123, 7758−7765

ported.[27−34] Experimental results demonstrate that morphology of the gold nanoclusters and dimers on a MgO surface and graphene can be controlled by applying electric field.[31,27] Reduction of an Ag-supported NiO film was found to take place under the applied electric field of ∼1 V nm^{-1}.[33] Hydrogen adsorption energy on doped graphene was shown to increase up to 0.3 eV under the electric field of 1 V $Å^{-1}$.[29] Furthermore, the electric field has been shown to control the magnetism of nanostructures.[28,30,34,32] All of these findings highlight the diverse impact of electric field on material's properties.

Herein, we systematically consider adsorption of CO_2, SO_2, and H_2CO molecules on both bulk and Mo-supported CaO films with varying thicknesses and as a function of the applied electric field. The motivation for using Mo is due to the experimental utilization as a support for CaO films and the overall enhancement of adsorption on metal oxide surfaces.[21,35,36] Considering the effects of an external electric field is relevant for interpreting results from scanning tunneling microscopy (STM) of small molecules on metal−supported oxide films, where the molecules to be probed may feel strong (of the order of 1 V/nm) electric fields induced by the STM tip.

2. COMPUTATIONAL DETAILS

2.1. Electronic Structure Calculations. All calculations were carried out by using the GPAW 1.1.0 code within the framework of density functional theory (DFT).[37] The Bayesian error estimation function with van der Waals correction (BEEF-vdW) was utilized.[38] The choice is due to the importance of correction for polarization and dispersion forces for description of interfaces.[39] This functional has been previously successfully used for oxide/metallic interfaces.[40,41] The core electrons of atoms were presented by PAW setups in the frozen-core approximation. A spin-unpolarized approach was employed for all calculations and wave functions were described in a real space grid with the maximum grid spacing of 0.20 Å. The reciprocal space was sampled with the (6 × 6 x 1) Monkhorst−Pack *k*-point mesh for the supported system. Each studied structure was allowed to relax until the maximum residue force was 0.05 eV $Å^{-1}$. The electric field was applied along the nonperiodic *z* direction and atomic charges were determined with the Bader scheme of charge density decomposition.[42−45] The adsorption energy, ΔE_{ads}, defined as the difference of total energies

$$\Delta E_{ads} = E(\text{ads/CaO/Mo}) - E(\text{CaO/Mo}) - E(\text{ads})$$

for the Mo-supported films and as

$$\Delta E_{ads} = E(\text{ads/CaO}) - E(\text{CaO}) - E(\text{ads})$$

for bulk and supported CaO models, where "ads" denotes the adsorbate. With this definition, a stronger adsorption energy is indicated by a more negative value of ΔE_{ads}.

2.2. Computational Models of Bulk and Mo Supported CaO films. Both unsupported and supported CaO films were modeled with the (2 × 2) surface cell. We employed a 4-layer thick Mo slab support, on which a thin, 3, 5 or 7, monolayer thick, CaO film was placed and oxide anions were aligned with the Mo atoms the CaO−Mo interface. The same film thicknesses were studied for free-standing films. The optimized lattice constant for CaO is 4.81 Å and that for Mo is 3.17 Å. In all calculations including the support metal, the theoretical Mo lattice constant was employed and the CaO structure was adapted to that. For free-standing CaO films, the optimized CaO lattice constant was used. Figure 1 illustrates

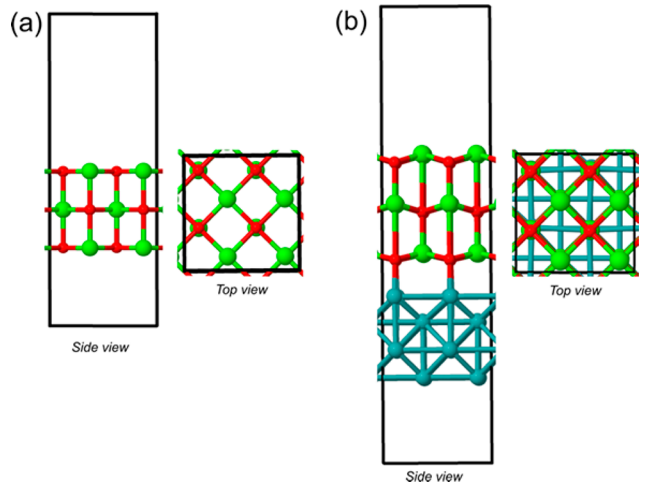

Figure 1. Structural models of (a) 3 ML thick bulk CaO film and (b) 3 ML thick CaO film supported by 4 ML Mo(100) used in the study (green, Ca; red, O; blue, Mo).

typical structure models used in the present study. In structure optimization, the two bottom-most Mo layers were frozen to their ideal bulk positions, while other atoms were free to relax. For unsupported CaO, either one or two bottom layers were frozen in the structure optimization depending on the film thickness. A sufficient amount of vacuum region was added above and below the slab to ensure the decay of the wave functions within the computational cell. We note that the applied electric field lowers the symmetry of CaO films due to the external perturbation and, therefore, makes the ions symmetrically inequivalent. We performed calculations for supported and unsupported films with and without adsorbates varying the value of the electric field in a stepwise manner from −2 to +2 V nm^{-1} in steps of 1 V nm^{-1}. The range of the external electric field values was selected according to typical experimental setups in STM studies.[2]

3. RESULTS AND DISCUSSION

The results will be discussed as follows. We start with adsorption characteristics of CO_2, SO_2, and H_2CO molecules on bulk and Mo-supported CaO films together with their electronic structure (in section 3.1) after which we address the adsorption energies and structure of the same set of models as a function of the applied electric field.

3.1. Adsorption of CO_2, SO_2, and H_2CO on Free-Standing and Mo-Supported CaO Films. First, we carefully explored all the possible adsorption structures of studied molecules on a 3 ML thick CaO film. Figure 2 summarizes all the adsorption structures identified for CO_2, SO_2, and H_2CO.

The two nearly equally exothermic CO_2 adsorption geometries on CaO are shown in Figure 2, parts a and b; the minor, 0.1 eV energy difference is due the orientation of oxygens in CO_2. The distance between the C atom and the O anion of the topmost CaO layer is 1.43 Å. Notably, the O−C−O angle of CO_2 in these adsorption structures is reduced from 180° for the gas-phase molecule to 130.2° and simultaneously the C−O distance is elongated from 1.16 to 1.26 Å. In the

DOI: 10.1021/acs.jpcc.8b06378
J. Phys. Chem. C 2019, 123, 7758−7765

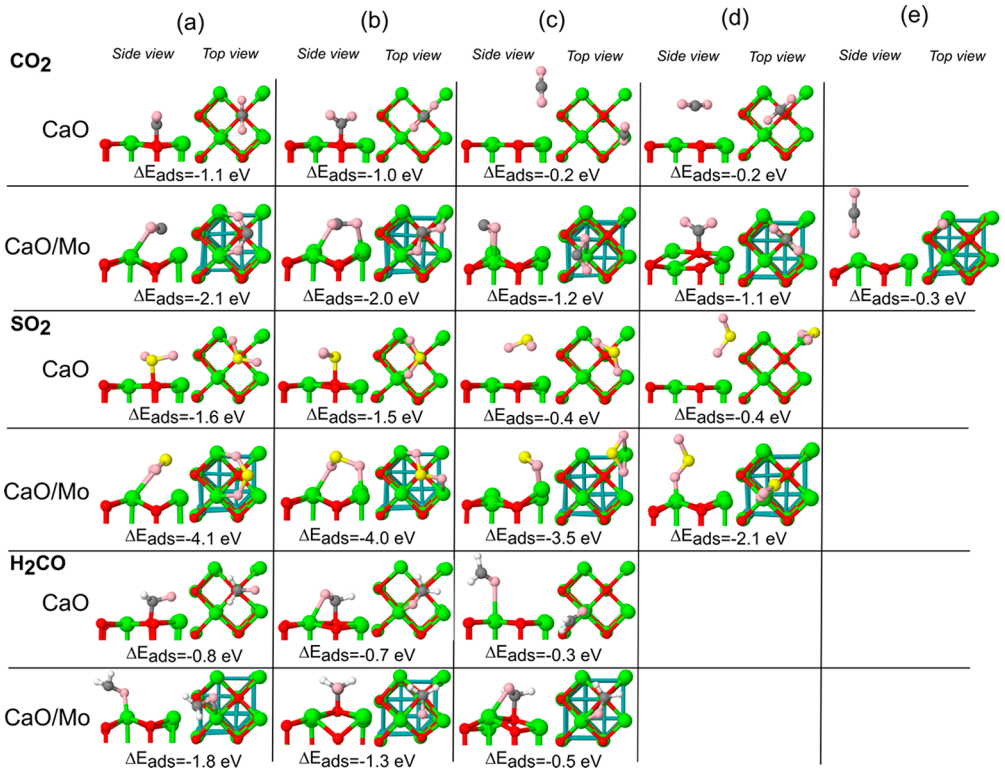

Figure 2. Adsorption structures and energies of CO_2, SO_2, and H_2CO molecules studied on 3 ML thick bulk and Mo-supported CaO films. Key: green, Mg; red, lattice O; pink, adsorbate O; gray, C; white, H.

presence of the Mo support, CO_2 favors an adsorption geometry (CaO/Mo, structure a), where the oxygen of CO_2 interacts with a Ca cation with the distance of 2.35 Å. A similar adsorption geometry to the most favorable bulk CO_2/CaO structure was also found for a CO_2/CaO/Mo system (d). However, it gives about same adsorption energy as on bulk CaO, which is 1 eV less exothermic than the best adsorption energy on the Mo-supported CaO. This geometry differs also significantly from the gas-phase structure since the O−C−O angle is 120.6° and the C−O bond length is 1.30 Å.

In the most favorable adsorption geometry, a SO_2 molecule binds from a S atom to a lattice anion of CaO (Figure 2(a) SO_2) with the S−O distance of 1.72 Å. Similar to CO_2, the structural properties of the molecule change compared to a gas-phase SO_2 molecule: O−S−O angle reduces from 119° to 111.4° and S−O distance elongates from 1.43 to1.51 Å. Again, the presence of a Mo support changes the best adsorption geometry of the molecule and the adsorption energy becomes more exothermic by 2.5 eV. The molecule binds now to a Ca cation from its oxygens with the O−Ca distance of 2.33 Å. The structural properties of SO_2 change also in this case, and the O−S−O angle becomes 108.2° and S−O bond length is as long as 1.62 Å indicating substantial activation of the molecule.

The third molecule that we consider is formaldehyde, which most stable adsorption geometries are shown in Figure 2. On bulk CaO(100) the most exothermic adsorption energy is −0.8 eV and H_2CO binds from the C atom to a lattice anion with the distance of 1.49 Å. In addition, C−H and C−O distances in H_2CO have changed compared to the values of a gas-phase molecule, 1.11 and 1.20 Å, to 1.30 and 1.33 Å for an adsorbed species. Similar to CO_2 and SO_2 adsorption, the presence of Mo support leads to the different formaldehyde adsorption geometries and energies compared to the bulk CaO surface. In the energetically best adsorption geometry H_2CO is bound from an oxygen atom to a Ca cation with both internal C−H and C−O bond lengths being 1.1 Å and the adsorption energy −1.8 eV, which is 1 eV more exothermic than that on CaO.

Figure 2 shows that the Mo support introduces significant structural changes in a CaO film. We studied the changes in atomic positions of Ca^{2+} and O^{2-} ions with respect to each other, that is, so-called rumpling of the CaO/Mo interface. We found that rumpling is ∼0.4 Å for the oxide−metal interface and ∼0.6 Å for the top CaO layer despite the film thickness. The rumpling results partly from the lattice mismatch between CaO and Mo but in experiments interdiffusion of Mo atoms into CaO films impact also on rumpling.[10,46] For unsupported CaO films, only minor rumpling, ∼ 0.03 and ∼0.02 Å for the bottom and topmost layers, respectively, was found.

Next, we considered adsorption on free-standing and Mo-supported CaO films with thicknesses of 5 ML, and 7 ML (Table 1) focusing on the most stable adsorption geometries on 3 ML thick oxide films. Since previous results highlight that the most favorable adsorption geometry of CO_2 on MgO/

Table 1. CO_2, SO_2, and H_2CO Adsorption Energies on 3, 5, 7 ML Layers Thick Mo-Supported CaO Films

	ΔE_{ads} (eV)		
	CO_2	SO_2	H_2CO
3 ML	−1.1	−1.6	−0.8
5 ML	−1.1	−1.6	−0.8
7 ML	−1.1	−1.6	−0.8
3 ML Mo	−2.1	−4.1	−1.8
5 ML Mo	−2.0	−4.0	−1.8
7 ML Mo	−2.0	−3.8	−1.7

DOI: 10.1021/acs.jpcc.8b06378
J. Phys. Chem. C 2019, 123, 7758−7765

Table 2. Bader Charges of Adsorbates, Distances between an Adsorbate and the Top CaO Layer for 3, 5, and 7 ML Thick Bulk and Mo-Supported CaO Films, and the CaO−Mo Interface Distance for the Supported System

	thickness					
	3 ML	5 ML	7 ML	3 ML CaO/Mo	5 ML CaO/Mo	7 ML CaO/Mo
CO_2 charge (|e|)	−0.45	−0.38	−0.47	−1.49	−1.39	−1.33
SO_2 charge (|e|)	−0.41	−0.37	−0.37	−1.44	−1.36	−1.27
H_2CO charge (|e|)	−0.36	−0.38	−0.33	−1.12	−1.11	−1.07
$d_{CO_2\text{-}CaO}$ (Å)	1.43	1.43	1.43	2.35	2.38	2.40
$d_{SO_2\text{-}CaO}$ (Å)	1.72	1.72	1.73	2.33	2.35	2.38
$d_{H_2CO\text{-}CaO}$ (Å)	1.49	1.49	1.49	2.33	2.34	2.35
$d_{Mo\text{-}CaO}$ (Å) (no adsorbate)	–	–	–	2.15	2.12	2.11
$d_{Mo\text{-}CaO}$ (Å) (CO_2)	–	–	–	2.07	2.08	2.09
$d_{Mo\text{-}CaO}$ (Å) (SO_2)	–	–	–	2.07	2.08	2.08
$d_{Mo\text{-}CaO}$ (Å) (H_2CO)	–	–	–	2.10	2.10	2.10
$d_{C-O}(CO_2)$ (Å)	1.26	1.26	1.26	1.30	1.29	1.28
angle O−C−O (CO_2)	130.2	130.0	130.0	120.6	122.5	123.9
$d_{S-O}(SO_2)$ (Å)	1.51	1.51	1.51	1.62	1.61	1.61
angle O−S−O (SO_2)	111.2	110.9	110.9	108.2	108.8	109.2
$d_{C-H}(H_2CO)$ (Å)	1.30	1.30	1.30	1.10	1.10	1.11
$d_{C-O}(H_2CO)$ (Å)	1.33	1.33	1.33	1.38	1.37	1.36

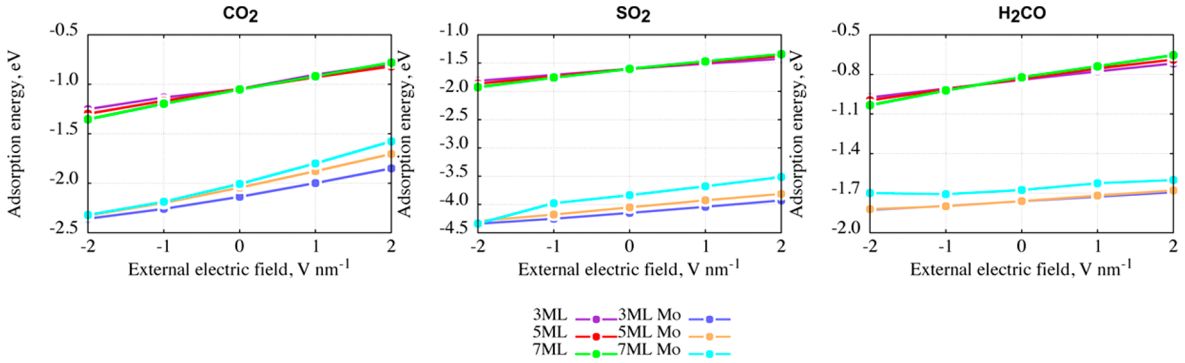

Figure 3. CO_2, SO_2, and H_2CO adsorption energies on 3, 5, 7 ML layers thick bulk and Mo-supported CaO film as a function of the applied electric field.

metal depends on the MgO film thickness,[47] we checked alternative, less stable, binding geometries, identified on 3 ML films, for CO_2 and SO_2 on 5 and 7 ML CaO models. On the basis of the obtained results, we can conclude that the same geometries represent the most stable interaction for all studied thicknesses.

Table 1 shows that on unsupported CaO films, adsorption energies are independent of the film thickness giving the same adsorption energies for all the studied thicknesses. However, a systematic effect on the film thickness is observed for CaO/Mo systems where the adsorption on the thinnest films is most exothermic. Overall, the adsorption energy of all molecules is significantly enhanced on Mo-supported films: 1.0 eV for CO_2, 2.5 eV for SO_2, and 1.0 eV for H_2CO for the 3 ML systems. It is interesting to note that this trend of enhanced adsorption energies follows quite closely to the known trend[48] of electron affinities of gas-phase molecules: −0.60, +1.11, and −0.65 eV for CO_2, SO_2, and H_2CO, respectively. We believe that the SO_2/CaO/Mo system behaves like a Lewis acid−base with Mo support functioning as the base.

In the following, we discuss structural and electronic parameters collected in Table 2. For all the studied adsorbates on free-standing CaO, the adsorption geometry and the molecule−oxide distance are independent of the film thickness and CO_2 resides closest to the surface while SO_2 is located nearly 0.3 Å further away. The Bader charge analysis shows minor variation in adsorbate charges as a function of film thickness, but in general, each molecule gains ∼−0.4 e, being almost neutral. Similarly, the variation of internal structural properties of adsorbed species are minor on unsupported films with different thicknesses, further supporting the finding that the adsorption energy remains the same on all film thicknesses

For CaO/Mo films, the presence of a Mo support introduces ∼1 Å increase into the molecule oxide distance but again the variation as a function of oxide film thickness is minor being at most ∼0.05 Å with increasing film thickness. The Mo−O interface distance depends slightly on the film thickness, while rumpling remains the same. The presence of an adsorbate decreases the interfacial distance but this is independent of the chemical nature of a molecule, e.g., ∼0.08 Å for 3 ML CaO/Mo, which is due to the polarization of the interfacial layer originating due to the charge transfer.[36] The Mo support also enhances charge transfer to the adsorbates so that CO_2 and SO_2 gain about 1 |e| and H_2CO about 0.7 |e|. These significant changes in charge state of the molecule due to the presence of the support are also reflected in internal structural properties of the molecules compared to the values on a bulk CaO surface. Interestingly, some internal structural properties depend on

DOI: 10.1021/acs.jpcc.8b06378
J. Phys. Chem. C 2019, 123, 7758−7765

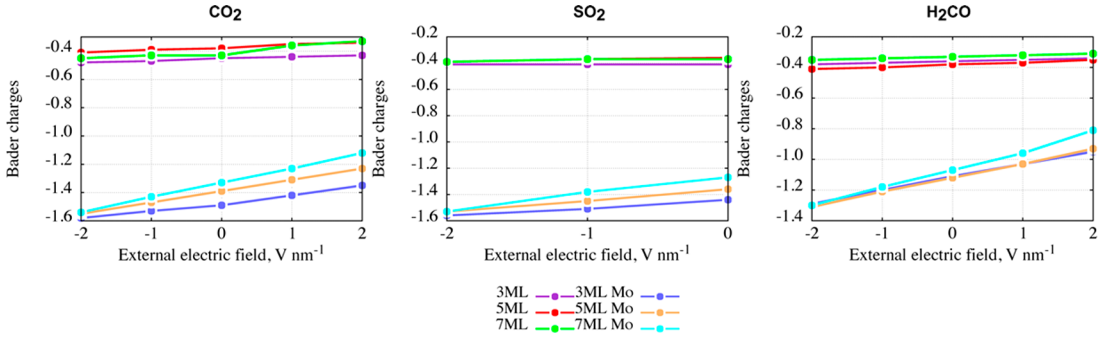

Figure 4. Bader charges of CO_2, SO_2, and H_2CO adsorbates on the 3, 5, and 7 ML thick bulk and Mo-supported CaO films as a function of the applied electric field.

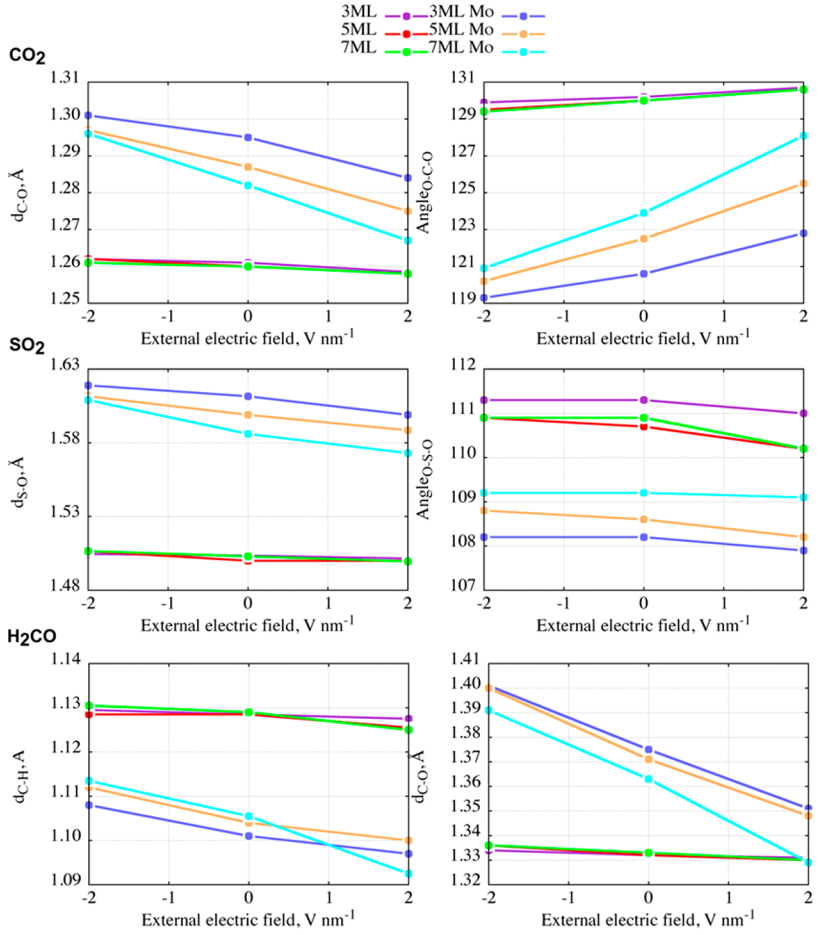

Figure 5. Change in geometries of CO_2, SO_2, and H_2CO molecules adsorbed on 3, 5, and 7 ML thick bulk and Mo-supported CaO films as a function of the applied electric field.

film thickness, e.g., the O−C−O angle in CO_2 increases from 120.6° on 3 ML CaO/Mo to 123.9° on 7 ML CaO/Mo. According to the Bader analysis, the charge gained by an adsorbate originates from Mo support, which has Bader charges of +1.1, + 0.9, and +0.8 e for 3, 5, and 7 ML thick CaO films, respectively. Upon increasing film thickness, the charge transfer to molecules correspondingly slightly decreases. Similar effect has been previously reported for NO_2 on metal−supported MgO.[36] Overall, our findings are in line with previous investigations on Au adsorption, where charge transfer decreases with increasing film thickness.[49]

3.2. Adsorption of CO_2, SO_2, and H_2CO on Bulk and Mo-Supported CaO Films as a Function of the Applied Electric Field.

We investigated the effect of the applied electric field on the adsorption energies of CO_2, SO_2, and H_2CO on both bulk and Mo-supported 3, 5, and 7 ML thick CaO films (Figure 3). All calculations were carried out only for energetically the most favorable structures found for 3 ML thick bulk and Mo-supported systems. We use a sign convention where positive values of the electric field indicate direction from Mo support to adsorbate, while negative values indicate the opposite direction.

A systematic reduction of the adsorption energy is detected for all the studied systems when the positive electric field is applied. In opposite, a systematic increase of the adsorption energy is seen when negative electric field is applied. Similar

DOI: 10.1021/acs.jpcc.8b06378
J. Phys. Chem. C 2019, 123, 7758−7765

effect was reported for the N-doped graphene interacting with hydrogen.[29] Therefore, such an effect of the electric field seems to lead to manipulation of the adsorption energy. Interestingly, CaO films without Mo support show thickness-independent behavior as in the absence of the electric field, giving almost identical adsorption energies. Also, Mo-supported systems typically show the same trend as in the absence of the electric field: thinner films have stronger interaction with adsorbates. Such results can be rationalized based on the obtained the Bader charges of adsorbates (Figure 4). We inspected systematic changes in the charges of adsorbates on CaO films with different thicknesses as a function of the applied electric field. In particular, increased intensity of the electric field in the negative polarity seems to lead to bigger charge transfer which, consequently, results in stronger adsorption energy. The changes in adsorbate charges can be explained by the direction of the applied electric field according to our convention, since the positive field pushes electrons from the adsorbate to the surface while the negative field attracts electrons to the adsorbate. A similar effect on the charge transfer depending on the direction of the electric was previously reported.[31]

Next, we looked at the local density of states with detailed consideration of 3 ML thick bulk and Mo-supported CaO films (Figure S1). We found that applied electric field depending on the direction leads to a small but systematic shift of the bands; positively applied electric field results in shift to the right, higher energy side, whereas a negatively applied electric field leads to an opposite shift of the bands to the left side. A similar effect of the band shift by the electric field was reported before.[31] These findings are interesting regarding interpretation of scanning tunneling spectroscopy (STS) results of adsorbates on oxides, since, routinely, the corresponding DFT modeling is done without the consideration of electric-field effects on the position of adsorbates electronic states in the oxide band gap. In typical STM/STS experiments the tip bias is in the range of 1−2 V nm^{-1} in both polarities.[50−52]

Rumpling of the interface layer for Mo-supported models with adsorbates under the applied electric field remains unchanged which is explained by the restraining effect of the metal support. Some changes are seen for bulk models, where rumpling under −2 and +2 V nm^{-1} intensity of the electric field results in up to ∼0.07 Å that is observed to be relatively large by taking into account that in the absence of the electric field it is ∼0.03 Å.

Next, we inspected distances between adsorbate and the topmost CaO layer as from Table 2, but only minor difference (<0.1 Å) was detected. Finally, we investigated change in adsorbate geometry depending on the applied electric field (Figure 5). We found that the electric-field effect on the adsorbate geometry is much stronger for Mo-supported models that is in line with calculated adsorption energies. A linear dependence of structural parameters on the applied electric field is clearly observed; it is particularly interesting to note that increasing the negative polarity of the field activates the double bonds of the adsorbates by elongating the C−O (in CO_2 and H_2CO) and S−O (in SO_2) bonds significantly.

4. CONCLUSIONS

We performed a systematic computational study by using density functional theory on the adsorption of CO_2, SO_2, and H_2CO molecules on both free-standing (bulk-like) and Mo-supported CaO films. Particular attention was paid to effects from an external electric field. The studied model systems are relevant for interpreting experimental results of imaging small molecules on metal−supported oxides via scanning tunneling microscopy.

The adsorption on Mo-supported CaO films is systematically stronger than on the corresponding free-standing CaO films, furthermore, the Mo support induces clear anionic charging of all of the adsorbates and changes their structures toward activated (longer) C−O/S−O bonds. The external electric field is shown to yield additional control of the adsorbate binding energy, charging, and structure, as it provides means to regulate primarily the adsorbate charge via "pushing/pulling" effects for electrons to/from the adsorbates. These effects are shown to be more dominant on thicker Mo-supported CaO films. This finding indicates that electric field effects could be utilized when designing nanocatalysts from modified oxides, particularly targeting C−O or S−O bond activation. Significant changes of adsorption energies as a function of the electric field strength were also observed, such as almost 1 eV change in the range of −2 to +2 eV/nm for both CO_2 and SO_2 on 7 ML CaO/Mo. This indicates that care should be exercised when interpreting imaging results from scanning tunneling microscopy and/or spectroscopy in experimental setups where the systems are scanned over a wide range of bias voltage, as the geometric or electronic structure of the adsorbate(s) may change appreciably in the scanning voltage window.

■ ASSOCIATED CONTENT

Supporting Information

The Supporting Information is available free of charge on the ACS Publications website at DOI: 10.1021/acs.jpcc.8b06378.

Additional data in Figure S1 (electronic density of states in 3 ML CaO and CaO/films) (PDF)

■ AUTHOR INFORMATION

Corresponding Author

*(H.H.) E-mail: hannu.j.hakkinen@jyu.fi.

ORCID

Mikhail S. Kuklin: 0000-0001-9289-6905
Karoliina Honkala: 0000-0002-3166-1077
Hannu Häkkinen: 0000-0002-8558-5436

Notes

The authors declare no competing financial interest.

■ ACKNOWLEDGMENTS

This work was financially supported by the Academy of Finland (Project 294217 and Academy Professorship to H.H.). Computer resources from Finnish IT Center for Science are gratefully acknowledged. We thank A. Bazhenov for useful discussions.

■ REFERENCES

(1) Freund, H. J.; Pacchioni, G. Oxide Ultra-Thin Films on Metals: New Materials for the Design of Supported Metal Catalysts. *Chem. Soc. Rev.* **2008**, *37*, 2224−2242.

(2) Nilius, N. Properties of Oxide Thin Films and Their Adsorption Behavior Studied by Scanning Tunneling Microscopy and Conductance Spectroscopy. *Surf. Sci. Rep.* **2009**, *64*, 595−659.

(3) Giordano, L.; Pacchioni, G. Oxide Films at the Nanoscale: New Structures, New Functions, and New Materials. *Acc. Chem. Res.* **2011**, *44*, 1244−1252.

DOI: 10.1021/acs.jpcc.8b06378
J. Phys. Chem. C 2019, 123, 7758−7765

(4) Honkala, K. Tailoring Oxide Properties: An Impact on Adsorption Characteristics of Molecules and Metals. *Surf. Sci. Rep.* **2014**, *69*, 366−388.
(5) Pacchioni, G.; Freund, H. Electron Transfer at Oxide Surfaces. The MgO Paradigm: From Defects to Ultrathin Films. *Chem. Rev.* **2013**, *113*, 4035−4072.
(6) Sterrer, M.; Risse, T.; Martinez Pozzoni, U.; Giordano, L.; Heyde, M.; Rust, H.-P.; Pacchioni, G.; Freund, H.-J. Control of the Charge State of Metal Atoms on Thin MgO Films. *Phys. Rev. Lett.* **2007**, *98*, 096107.
(7) Prada, S.; Giordano, L.; Pacchioni, G. Charging of Gold Atoms on Doped MgO and CaO: Identifying the Key Parameters by DFT Calculations. *J. Phys. Chem. C* **2013**, *117*, 9943−9951.
(8) Pacchioni, G.; Giordano, L.; Baistrocchi, M. Charging of Metal Atoms on Ultrathin MgO/Mo(100) Films. *Phys. Rev. Lett.* **2005**, *94*, 226104.
(9) Frondelius, P.; Hellman, A.; Honkala, K.; Häkkinen, H.; Grönbeck, H. Charging of Atoms, Clusters, and Molecules on Metal-Supported Oxides: A General and Long-Ranged Phenomenon. *Phys. Rev. B: Condens. Matter Mater. Phys.* **2008**, *78*, 085426.
(10) Shao, X.; Myrach, P.; Nilius, N.; Freund, H. J. Growth and Morphology of Calcium-Oxide Films Grown on Mo(001). *J. Phys. Chem. C* **2011**, *115*, 8784−8789.
(11) Pacchioni, G.; Sousa, C.; Illas, F.; Parmigiani, F.; Bagus, P. S. Measures of Ionicity of Alkaline-Earth Oxides from the Analysis of Ab Initio Cluster Wave Functions. *Phys. Rev. B: Condens. Matter Mater. Phys.* **1993**, *48*, 11573.
(12) Pacchioni, G.; Ricart, J. M.; Illas, F. Ab Initio Cluster Model Calculations on the Chemisorption of CO_2 and SO_2 Probe Molecules on MgO and CaO (100) Surfaces. A Theoretical Measure of Oxide Basicity. *J. Am. Chem. Soc.* **1994**, *116*, 10152−10158.
(13) Chiesa, M.; Giamello, E.; Murphy, D. M.; Pacchioni, G.; Paganini, M. C.; Soave, R.; Sojka, Z. Reductive Activation of the Nitrogen Molecule at the Surface Of "Electron-Rich" MgO and CaO. The N_2^- Surface Adsorbed Radical Ion. *J. Phys. Chem. B* **2001**, *105*, 497−505.
(14) Nikulshina, V.; Gebald, C.; Steinfeld, A. CO_2 Capture from Atmospheric Air via Consecutive CaO-Carbonation and $CaCO_3$-Calcination Cycles in a Fluidized-Bed Solar Reactor. *Chem. Eng. J.* **2009**, *146*, 244−248.
(15) Wang, S.; Yan, S.; Ma, X.; Gong, J. Recent Advances in Capture of Carbon Dioxide Using Alkali-Metal-Based Oxides. *Energy Environ. Sci.* **2011**, *4*, 3805−3819.
(16) Choi, S.; Drese, J. H.; Jones, C. W. Adsorbent Materials for Carbon Dioxide Capture from Large Anthropogenic Point Sources. *ChemSusChem* **2009**, *2*, 796−854.
(17) Speight, J. G. *The Chemistry and Technology of Petroleum*, 2nd ed.; Dekker: New York, 1991.
(18) Bartholomew, C. H.; Agrawal, P. K.; Katzer, J. R. Sulfur Poisoning of Metals. *Adv. Catal.* **1982**, *31*, 135−142.
(19) Rodriguez, J. A.; Hrbek, J. Interaction of Sulfur with Well-Defined Metal and Oxide Surfaces: Unraveling the Mysteries Behind Catalyst Poisoning and Desulfurization. *Acc. Chem. Res.* **1999**, *32*, 719−728.
(20) Besson, R.; Rocha Vargas, M.; Favergeon, L. Surface Science CO_2 Adsorption on Calcium Oxide: An Atomic-Scale Simulation Study. *Surf. Sci.* **2012**, *606*, 490−495.
(21) Solis, B. H.; Cui, Y.; Weng, X.; Seifert, J.; Schauermann, S.; Sauer, J.; Shaikhutdinov, S.; Freund, H.-J. Initial Stages of CO_2 Adsorption on CaO: A Combined Experimental and Computational Study. *Phys. Chem. Chem. Phys.* **2017**, *19*, 4231−4242.
(22) Voigts, F.; Bebensee, F.; Dahle, S.; Volgmann, K.; Maus-Friedrichs, W. The Adsorption of CO_2 and CO on Ca and CaO Films Studied with MIES, UPS and XPS. *Surf. Sci.* **2009**, *603*, 40−49.
(23) Rodriguez, J. A.; Jirsak, T.; Freitag, A.; Larese, J. Z.; et al. Interaction of SO_2 with MgO (100) and Cu/MgO (100): Decomposition Reactions and the Formation of SO_3 and SO_4. *J. Phys. Chem. B* **2000**, *104*, 7439−7448.
(24) Peng, X.; Barteau, M. Adsorption of Formaldehyde on Model Magnesia Surfaces: Evidence for the Cannizzaro Reaction. *Langmuir* **1989**, *5*, 1051−1056.
(25) Kakkar, R.; Kapoor, P. N.; Klabunde, K. J. Theoretical Study of the Adsorption of Formaldehyde on Magnesium Oxide Nanosurfaces: Size Effects and the Role of Low-Coordinated and Defect Sites. *J. Phys. Chem. B* **2004**, *108*, 18140−18148.
(26) Kuklin, M. S.; Bazhenov, A. S.; Honkala, K.; Tosoni, S.; Pacchioni, G.; Häkkinen, H. Structure and Dynamics of CaO Films: A Computational Study of an Effect of External Static Electric Field. *Phys. Rev. B: Condens. Matter Mater. Phys.* **2017**, *95*, 165423.
(27) Yoon, B.; Landman, U. Electric Field Control of Structure, Dimensionality, and Reactivity of Gold Nanoclusters on Metal-Supported MgO Films. *Phys. Rev. Lett.* **2008**, *100*, 056102.
(28) Negulyaev, N. N.; Stepanyuk, V. S.; Hergert, W.; Kirschner, J. Electric Field as a Switching Tool for Magnetic States in Atomic-Scale Nanostructures. *Phys. Rev. Lett.* **2011**, *106*, 037202.
(29) Lee, S.; Lee, M.; Chung, Y.-C. Enhanced Hydrogen Storage Properties under External Electric Fields of N-Doped Graphene with Li Decoration. *Phys. Chem. Chem. Phys.* **2013**, *15*, 3243−3248.
(30) Liang, S. H.; Tao, L. L.; Liu, D. P.; Han, X. F. External Electric Field Effects on Electronic and Magnetic Properties at Molecule-Metal Interfaces: Cu-Phthalocyanine Adsorbed on Fe(001) Surface. *J. Appl. Phys.* **2013**, *114*, 083702.
(31) Zhou, X. H.; Huang, Y.; Chen, X. S.; Lu, W. External Electric Field Modulation of Structural Configurations and Electronic Properties of Gold Dimers on Graphene. *J. Phys. Chem. C* **2012**, *116*, 7393−7398.
(32) Juárez-Reyes, L.; Stepanyuk, V. S.; Pastor, G. M. Electric-Field-Modulated Exchange Coupling within and between Magnetic Clusters on Metal Surfaces: Mn Dimers on Cu(1 1 1). *J. Phys.: Condens. Matter* **2014**, *26*, 176003.
(33) Steurer, W.; Surnev, S.; Netzer, F. P.; Sementa, L.; Negreiros, F. R.; Barcaro, G.; Durante, N.; Fortunelli, A. Redox Processes at a Nanostructured Interface under Strong Electric Fields. *Nanoscale* **2014**, *6*, 10589−10595.
(34) Yun, K. H.; Lee, M.; Chung, Y. C. Electric Field as a Novel Switch for Magnetization of Fe/graphene System. *J. Magn. Magn. Mater.* **2014**, *362*, 93−96.
(35) Cui, Y.; Pan, Y.; Pascua, L.; Qiu, H.; Stiehler, C.; Kuhlenbeck, H.; Nilius, N.; Freund, H. J. Evolution of the Electronic Structure of CaO Thin Films Following Mo Interdiffusion at High Temperature. *Phys. Rev. B: Condens. Matter Mater. Phys.* **2015**, *91*, 035418.
(36) Grönbeck, H. Mechanism for NO_2 Charging on Metal Supported MgO. *J. Phys. Chem. B* **2006**, *110*, 11977−11981.
(37) Enkovaara, J.; Rostgaard, C.; Mortensen, J. J.; Chen, J.; Dułak, M.; Ferrighi, L.; Gavnholt, J.; Glinsvad, C.; Haikola, V.; Hansen, H. A.; et al. Electronic Structure Calculations with GPAW: A Real-Space Implementation of the Projector Augmented-Wave Method. *J. Phys.: Condens. Matter* **2010**, *22*, 253202.
(38) Wellendorff, J.; Lundgaard, K. T.; Møgelhøj, A.; Petzold, V.; Landis, D. D.; Nørskov, J. K.; Bligaard, T.; Jacobsen, K. W. Density Functionals for Surface Science: Exchange-Correlation Model Development with Bayesian Error Estimation. *Phys. Rev. B: Condens. Matter Mater. Phys.* **2012**, *85*, 235149.
(39) Chen, H.-Y. T.; Giordano, L.; Pacchioni, G. Adsorption Properties of Two-Dimensional NaCl: A Density Functional Theory Study of the Interaction of Co, Ag, and Au Atoms with NaCl/Au(111) Ultrathin Films. *J. Phys. Chem. C* **2014**, *118*, 12353−12363.
(40) Thirumalai, H.; Kitchin, J. R. The Role of vdW Interactions in Coverage Dependent Adsorption Energies of Atomic Adsorbates on Pt(111) and Pd(111). *Surf. Sci.* **2016**, *650*, 196−202.
(41) Wellendorff, J.; Silbaugh, T. L.; Garcia-Pintos, D.; Norskov, J. K.; Bligaard, T.; Studt, F.; Campbell, C. T. A Benchmark Database for Adsorption Bond Energies to Transition Metal Surfaces and Comparison to Selected DFT Functionals. *Surf. Sci.* **2015**, *640*, 36−44.
(42) Bader, R. F. W. A Quantum Theory of Molecular Structure and Its Applications. *Chem. Rev.* **1991**, *91*, 893−928.

DOI: 10.1021/acs.jpcc.8b06378
J. Phys. Chem. C 2019, 123, 7758−7765

(43) Henkelman, G.; Arnaldsson, A.; Jónsson, H. A Fast and Robust Algorithm for Bader Decomposition of Charge Density. *Comput. Mater. Sci.* **2006**, *36*, 354−360.
(44) Sanville, E.; Kenny, S. D.; Smith, R.; Henkelman, G. Improved Grid-Based Algorithm for Bader Charge Allocation. *J. Comput. Chem.* **2007**, *28*, 899−908.
(45) Tang, W.; Sanville, E.; Henkelman, G. A Grid-Based Bader Analysis Algorithm without Lattice Bias. *J. Phys.: Condens. Matter* **2009**, *21*, 084204.
(46) Shao, X.; Nilius, N.; Myrach, P.; Freund, H. J.; Martinez, U.; Prada, S.; Giordano, L.; Pacchioni, G. Strain-Induced Formation of Ultrathin Mixed-Oxide Films. *Phys. Rev. B: Condens. Matter Mater. Phys.* **2011**, *83*, 245407.
(47) Tosoni, S.; Spinnato, D.; Pacchioni, G. DFT Study of CO_2 Activation on Doped and Ultrathin MgO Films. *J. Phys. Chem. C* **2015**, *119*, 27594−27602.
(48) https://cccbdb.nist.gov/.
(49) Honkala, K.; Häkkinen, H. Au Adsorption on Regular and Defected Thin MgO(100) Films Supported by Mo. *J. Phys. Chem. C* **2007**, *111*, 4319−4327.
(50) Walter, M.; Frondelius, P.; Honkala, K.; Häkkinen, H. Electronic Structure of MgO-Supported Au Clusters: Quantum Dots Probed by Scanning Tunneling Microscopy. *Phys. Rev. Lett.* **2007**, *99*, 096102.
(51) Lin, X.; Nilius, N.; Sterrer, M.; Koskinen, P.; Häkkinen, H.; Freund, H. J. Characterizing Low-Coordinated Atoms at the Periphery of MgO-Supported Au Islands Using Scanning Tunneling Microscopy and Electronic Structure Calculations. *Phys. Rev. B: Condens. Matter Mater. Phys.* **2010**, *81*, 153406.
(52) Lin, X.; Nilius, N.; Freund, H. J.; Walter, M.; Frondelius, P.; Honkala, K.; Häkkinen, H. Quantum Well States in Two-Dimensional Gold Clusters on MgO Thin Films. *Phys. Rev. Lett.* **2009**, *102*, 206801.

DOI: 10.1021/acs.jpcc.8b06378
J. Phys. Chem. C 2019, 123, 7758−7765